Chapter 2

Architecture of Rafts

In this chapter we will be engaged in determining, in a non-invasive way, the organisation of specific lipids and proteins on the cell surface and whether the cell makes use of this organisation for specific functions. From our discussion in the first chapter, it is clear that any kind of organisation on the cell surface, if it were to exist, has to be of a size much smaller than the resolution of the optical microscope. We shall describe a fluorescence spectroscopic method which in conjunction with detailed theoretical modeling, will allow us to arrive at a quantitative understanding of protein-lipid organisation in rafts. We shall discuss the processes by which fluorophores attached to the proteins depolarise an incident beam of polarised light. Depolarisation is the prime observable that bears the stamp of molecular organisation at the nanometre scale. To this end, we begin with a short discussion of fluorescence, and then summarize Forster's theory of fluorescence resonance energy transfer (FRET) among neighbouring fluorophores; the probability of resonance depends on the local organisation of fluorophores and therefore can be used as a spectroscopic ruler (Stryer; 1978).

2.1 Elements of fluorescence

Following excitation from an incident beam of light, the emission of light from an electronically excited state is divided into two categories, *fluorescence* and phosphorescence, depending on the nature of the excited state (Lakowicz; 1999). In excited singlet states (S_1 or S_2), the electron in the higher orbital has a spin opposite to that of its partner in the ground-state orbital (S_0). Consequently the electron can return to the ground state by emitting a photon without violating Pauli's exclusion principle. The typical lifetime of fluorescence is $\tau \sim 10^{-8}$ s (Figure 2.1).

Phosphorescence involves the transition of an electron in a triplet excited state to the ground state, which is always singlet. In a triplet state the electron has the same spin as its partner in the ground level, so the transition is extremely slow, typical phosphorescence lifetimes varying from milliseconds to seconds.

The transition of an electron from S_0 to S_1 or S_2 takes about 10^{-15} s, an interval too

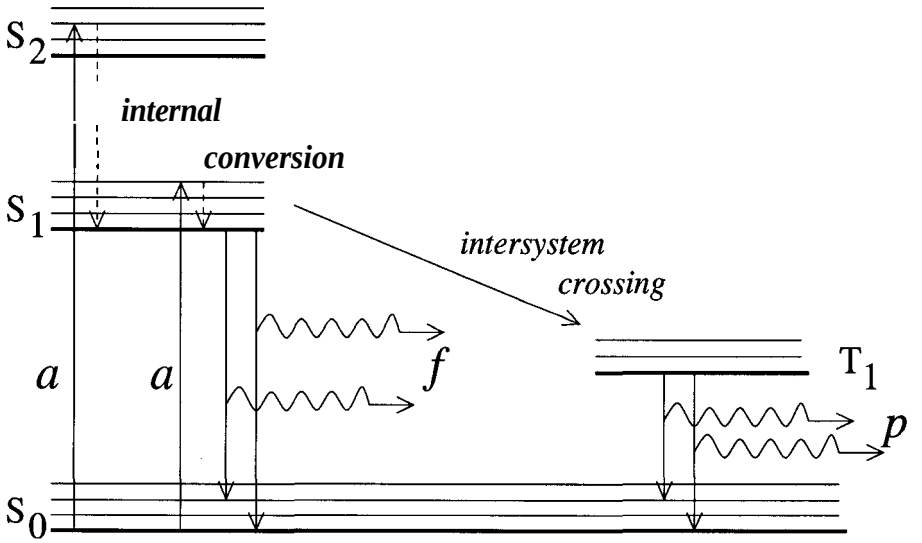

Figure 2.1: Electronic transitions leading to fluorescence and phosphorescence. The thick horizontal lines represent the lowest vibrational energy levels of the ground state, S_0, the first and the second excited singlet states, S_1 and S_2, and the triplet state, T_1. a, f and p refer to absorption of radiation, fluorescence and phosphorescence respectively. The phenomenon of intersystem crossing that leads an excited fluorophore to a very long-lived phosphorescent state will not be encountered in this thesis.

short for the nuclei of the constituent atoms of the fluorophore to change their positions. After the absorption of radiation, the electron is usually transferred not to the lowest level of S_1 or S_2 but to a higher vibrational level. The fluourophore quickly relaxes to the lowest vibrational level of S_1, this process is called internal conversion and is over in less than 10^{-12} s. Since τ is of the order of 10^{-8} s, internal conversion is complete prior to fluorescence.

Return to the ground state typically occurs through a higher vibrational level of S_0, after which the system reaches thermal equilibrium in about 10^{-12} s.

Quenching reduces the intensity of fluorescence by various means. Collisional quenching occurs when the fluorophore in an excited state is deactivated upon contact with another molecule in the solution. Static quenching refers to the process of the fluorophore in the ground state forming a nonfluorescent complex with another molecule.

2.2 Non-radiative transfer of electronic excitation

If an excited fluorophore is in proximity to another in the ground state then, under certain circumstances, the excitation can be passed to the latter without an emission of a photon. This process is called resonance. Resonance between the donor of energy (D) and the acceptor (A) occurs through the electrostatic interaction of the transition dipole moments ($\vec{p_D}$ and $\vec{p_A}$) of D and A. Forster's theory shows that if D and A are separated

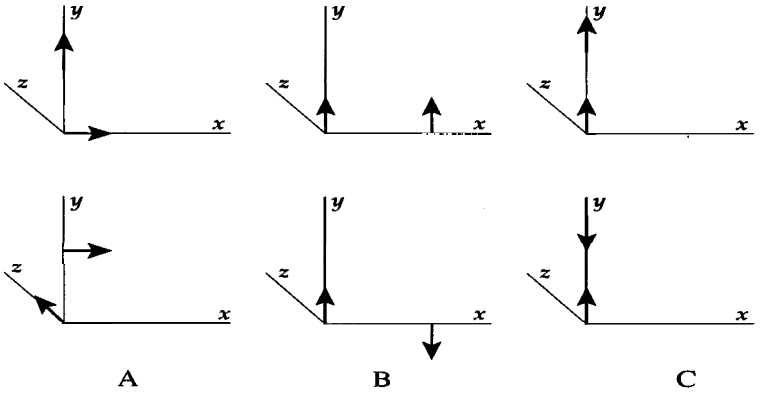

Figure 2.2: Even for a fixed separation between the donor and the acceptor, the probability of resonance depends on the relative orientation of $\vec{p_D}$ and $\vec{p_A}$ (thick arrows) because of the dipolar nature of the resonance interaction. Columns A, B and C represent relative orientations of the dipole moments for which κ^2 assumes the values 0, 1 and 4 respectively.

by a distance R then

$$\frac{\tau_{DA}}{\tau_0} = \frac{R^6}{R^6 + \kappa^2 R_0^6} \tag{2.1}$$

where τ_0 is the lifetime of fluorescence of an isolated fluorophore and τ_{DA} is the lifetime of the excited state of D in the presence of A (Forster; 1948). The dimensionless parameter κ^2, varying from 0 to 4, is governed by the relative orientations of the dipole moments of D and A and not by the distance between them (Figure 2.2). The Forster radius, R_0, is a fixed length determined by the spectral properties of the fluorophore and the refractive index of the medium in which D and A are immersed.

If an isolated fluorophore is excited at the initial instant of time then the probability that the energy is spontaneously emitted in the interval of time t to t + dt is given by the poisson distribution $\frac{dt}{\tau_0}\exp(-\$)$. Let us now take a pair of fluorophores and excite one of them at the initial instant. The probability that the fluorophore spontaneously emits its energy in the interval t to t + dt without ever transferring the energy to its partner is $\frac{dt}{\tau_0}\exp(-\frac{t}{\tau_0})\exp(-\mathrm{Wt})$.

$$W = \frac{3}{2}\kappa^2 \left(\frac{R}{R_0}\right)^6 \frac{1}{\tau_0} \tag{2.2}$$

$$R_0 = (8.79 \times 10^{-5} \times J \times \frac{2}{3} \times Q \times n^{-4})^{\frac{1}{6}} \mathring{A} \tag{2.3}$$

where Q is the quantum yield of fluorescence and n the refractive index. The spectral overlap J is calculated from the emission spectrum (f) and the absorption spectrum (ϵ) of the fluorophore,

$$J = \frac{\int d\lambda f(\lambda)\epsilon(\lambda)\lambda^4}{\int d\lambda f(\lambda)} \tag{2.4}$$

The orientation factor,

$$\kappa^2 = ((\vec{p_1} \cdot \vec{p_2}) - 3(\vec{p_1} \cdot \vec{e})(\vec{p_2} \cdot \vec{e}))^2, \tag{2.5}$$

where $\vec{e}$ is a unit vector joining the pair of fluorophores, their transition dipole moments aiming along the unit vectors $\vec{p_1}$ and $\vec{p_2}$. As we mentioned before, κ^2 contains all the

information regarding the relative orientation of the transition dipole moments of the fluorophores.

Therefore the probability of the excitation never being transferred non-radiatively from the excited fluorophore to its partner is

$$s_0 = \int_0^\infty \frac{dt}{\tau_0} \exp(-t/\tau_0) \exp(-Wt) = \frac{1}{1 + W\tau_0} \tag{2.6}$$

In order to extend this calculation to a larger population, we label the sole fluorophore excited by the incident radiation 0, and the neighbouring ones 1, 2, **3,** ..., N. The probability of 0 never transferring its energy to its neighbours is

$$s_0 = \int_0^\infty \frac{dt}{\tau_0} \exp(-t/\tau_0) \exp(-W_1 t) \exp(-W_2 t) \ldots \exp(-W_N t) = \frac{1}{1 + W\tau_0} \tag{2.7}$$

$$W = W_1 + W_2 + \ldots + W_N \tag{2.8}$$

For any fluorophore i, the corresponding W_i is calculated in a pairwise fashion — ignoring the presence of all but 0 and i. Thus we have to substitute $|\vec{R}_i - \vec{R}_0|$ for R in Equation 2.2 and put $\vec{p_1} = \vec{p_0}$, $\vec{p_2} = \vec{p_i}$ in Equation 2.5 to get W_i.

However 0 can spontaneously emit the energy even if it had transferred the energy to one of its neighbours, provided the neighbour returns the energy to 0. So we have to estimate r_i, the probability of 0 transferring its energy to i. Clearly,

$$r_1 + r_2 + \ldots + r_N = 1 - s_0 \tag{2.9}$$

because if 0 has not decayed spontaneously to its ground state then it must have transferred its energy to any one of its neighbours. Let us assume that

$$r_i = \frac{W_i}{W}(1 - s_0) \tag{2.10}$$

We thus have an expression of the probability of non-radiative transfer between any pair in an assembly of fluorophores.

Having arrived at an estimate of the likelihood of an excited fluorophore transmitting the excitation to a neighbour, we shall look for a means of observing such a resonance in an experimental system. We have two ways to that end :

- frequency selection
- polarisation selection

We shall consider each of these in turn.

The spectrum of radiation spontaneously emitted by any molecule is always red-shifted relative to the spectrum of the radiation that excited the molecule from the ground state (Figure **2.3).** This fact has been utilised in estimating the degree of resonance in an assembly of fluorophores consisting of two species — the donor and the acceptor. The

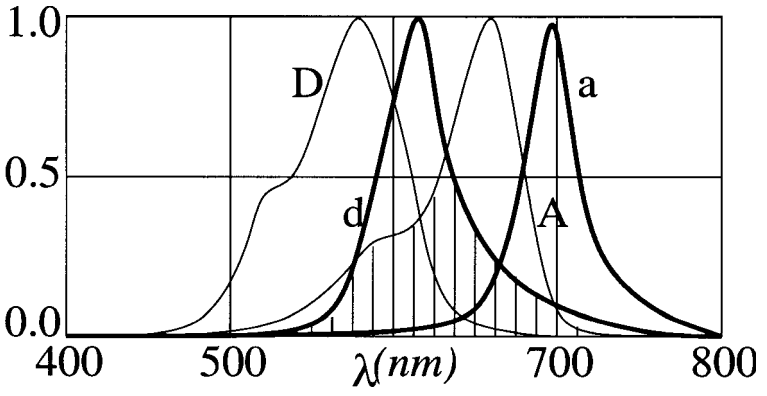

Figure 2.3: Variation with wavelength of the normalised rates of absorption and emission for the pair of fluorophores used in our experiments as the donor and the acceptor. (D,d) and (A,a) correspond to absorption and emission by the donor and the acceptor respectively. The overlap integral, **J**, is a measure of the area bounded by the graphs d and A, the striped region.

emission spectrum of the donor (f_D) partially overlaps the absorption spectrum of the acceptor (ϵ_A) but does not overlap at all with the emission spectrum of the acceptor. If on this system we shine light that falls entirely in the absorption spectrum of the donor and filter the fluorescence to capture light entirely in the emission spectrum of the acceptor then the strength of the signal is evidently a measure of the resonance between the two species of fluorophores. This resonance depends on the distance between the donor and the acceptor and the relative orientation of their dipole moments in exactly the same way as described earlier; in order to obtain the Forster radius we merely have to substitute f $= f_D$ and $\epsilon = \epsilon_A$ in Equations **2.3** and 2.4.

Though relatively simple to implement this is an inefficient method of detecting resonance. The signal records the transfer of energy from one group of fluorophores, the donors, to another group, the acceptors — it does not tell us how many times has the energy been passed from one molecule to another within the group of donors before being absorbed by an acceptor. Nor does it tell us anything about the possible hopping of the excitation within the group of acceptors before being finally released from the system. Therefore this method tends to underestimate the degree of resonance in the system.

So we turn to a property of radiation that is liable to change even in a single event of energy transfer — its polarisation. The radiation from a dipole moment is always polarised in the plane containing the axis of the dipole and the direction of propagation of the radiation. Suppose we have a pair of dipoles, 1 and 2, separated by a distance R, and 1 has been excited by an incident beam of polarised light. If R is not much greater then R_0 then there is an appreciable probability of 1 transferring its energy to 2 even if $\vec{p_1}$ and $\vec{p_2}$ are not parallel to one another — in fact the probability is proportional to κ^2 defined in Equation 2.5. Therefore if **2** releases the energy after borrowing it from **1** then we expect the light to be more depolarised than if **1** had released the energy without transferring it to 2.

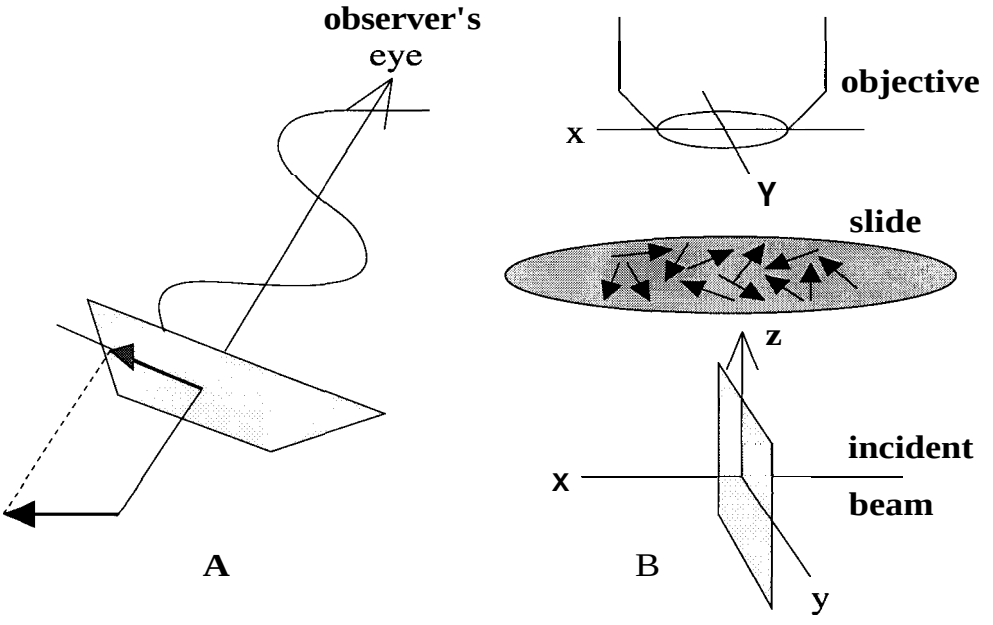

Figure 2.4: (A) To the observer the radiation from the dipole at the bottom is polarised in a plane containing the line of sight and the axis of the dipole — hence the observer will see an effective dipole moment that is a foreshortened form of the original one, being projected on to the plane perpendicular to the line of sight. (B) Schematic of the experimental set-up — the shaded plane is the plane of polarisation of the incident beam; the tiny arrows on the slide represent the dipole moments of the fluorophores; the polariser and the analyser on the objective allow us to collect light polarised either along the x axis or along the y axis.

First we need to know the extent of depolarisation of the incident beam brought about solely by the excitation and spontaneous emission of a lone fluorophore due to brownian rotation in a solvent of viscosity η. If the incident beam be polarised along the y axis then p_y^2 is the probability that the beam excites the fluorophore — $\vec{p}$ being a unit vector aiming along the transition moment of the fluorophore. Having been excited by the incident beam, the probability of spontaneously emitting light polarised along the x, y or z axis will be p_x^2, p_y^2 and p_z^2 respectively (Figure 2.4). If I_x and I, denote the intensity of the emitted light polarised along the x and y axis respectively, then the anisotropy is defined to be

$$A = \frac{I_y - I_x}{I_y + 2I_x} \tag{2.11}$$

Keeping the polarization of the incident beam fixed (along the y axis), we calculate the anisotropy:

$$A = \frac{< p_y^2 p_y^2 > - < p_y^2 p_x^2 >}{< p_y^2 p_y^2 > + 2 < p_y^2 p_x^2 >} \tag{2.12}$$

The angular brackets represent the mean over all possible orientations of the dipole. It is a simple exercise to show that A = 0.4 if $\vec{p}$ is uniformly distributed over a sphere (Agranovich and Galanin; 1982).

In the same spirit we can calculate the anisotropy if the incident beam excites 1 and 1

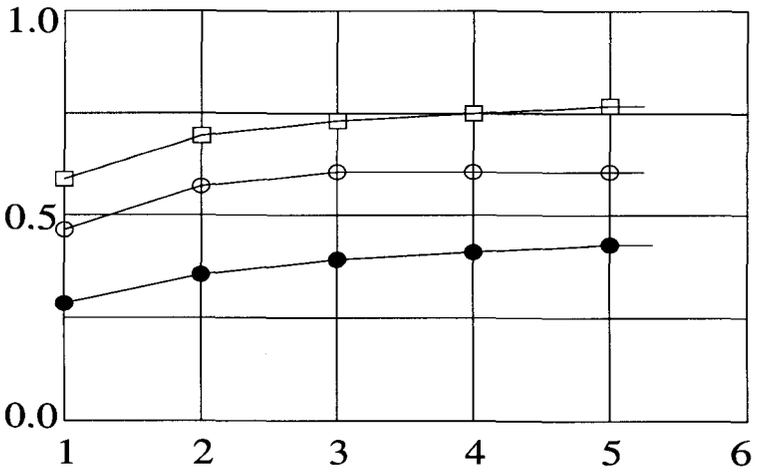

Figure 2.5: Probability of spontaneous emission from the initially excited fluorophore plotted against the maximum number of allowed transfers: full circle — q = 1.5; open circle — q = 1.0; square — q = 0.5.

transfers its energy to 2 while 2 emits the energy spontaneously. Obviously, in this case,

$$I_x \sim< p_{1y}^2 \kappa^2 p_{2x}^2 >, I_y \sim< p_{1y}^2 \kappa^2 p_{2y}^2 > \tag{2.13}$$

The mean has to be taken not only over all possible orientations of $\vec{p_1}$ and $\vec{p_2}$ but also over all possible orientations of $\vec{\epsilon}$, the unit vector joining 1 and **2.** Again it is a straight forward exercise to show that $\boldsymbol{A} = 0.016$ if $\vec{p_1}$ and $\vec{p_2}$ are uniformly distributed over a sphere and $\vec{\epsilon}$ is uniformly distributed over a unit circle (Agranovich and Galanin; 1982). Just a single transfer is enough to depolarise the light almost completely.

In order to simulate the process of energy transfer on a plane membrane we place the fluorophore 0 at the origin of coordinates. Let us set our unit of length at $R_0 = 1$; we take a square of side 6 units on the x-y plane with 0 at the centre, and distribute 1, 2, **3,** ..., N with uniform randomness over the square. The dipole moments of 0, 1, 2, ..., N are oriented with uniform randomness over a unit sphere. The positions of the fluorophores as well as the orientation of their dipole moments do not change with time. Assuming that 0 and only 0 has been excited by the incident radiation, we would first like to know the probability of spontaneous emission from 0 taking multiple transfer into account. The result is shown in Figure 2.5 where different plots correspond to different densities of fluorophores (measured by q, the average number of fluorophores in a circle of radius R_0). In the rest of the simulation we will include a maximum of four events of energy transfer.

We start with 0 in the excited state and calculate, according to the formula we have established, the probability of 0 emitting spontaneously (s_0) or transferring the energy to n *(r,),* where n can vary from 1 to N. The actual outcome is determined by calling a random number $(t)$with uniform distribution from 0 to 1. If t is smaller than s_0 then the outcome is spontaneous emission from 0, if t is between s_0 and $s_0 + r_1$ then the outcome is a transfer from 0 to 1, and so on. If the outcome is spontaneous emission from 0, then

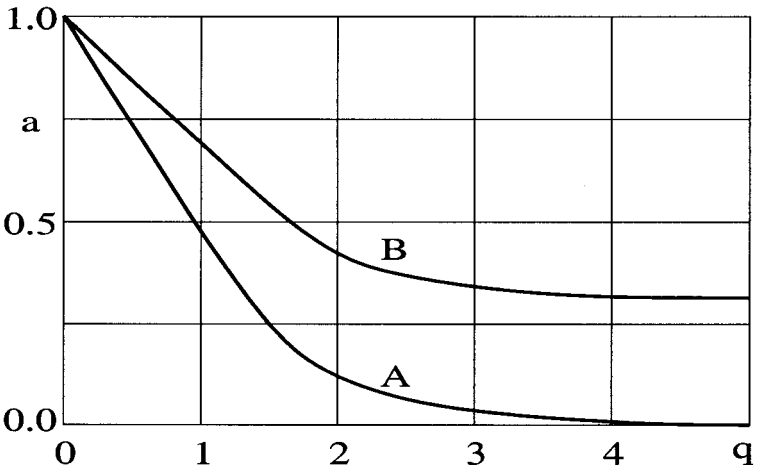

Figure 2.6: Relative anisotropy ($a = F(q, \mathrm{J})$) plotted against the concentration of fluorophores: (A) $\xi = 0.0$, (B) $\xi = 0.8$. Averaged over 7500 trials.

we record, for this trial, the anisotropy to be A_0, where

$$A_m = \frac{p_{my}^2 - p_{mx}^2}{p_{my}^2 + 2p_{mx}^2}, (m = 0, 1, 2, \ldots, N). \tag{2.14}$$

Or else, if 0 transfers its energy to n, then we repeat the calculation, this time n as the donor and all the rest (0, 1, ..., n – 1, n + 1, ..., N) as acceptors. Proceeding in this fashion, if at any stage the outcome be a spontaneous emission from m, we record, for this trial, the anisotropy to be A$_m$. We repeat the trial many times, always starting with 0 as the initially excited fluorophore, and record the anisotropy for each trial. The mean of the anisotropy, over all the trials, stands for a measurement of the anisotropy in a real experiment.

We may now study the effect of orientational correlation among the dipole moments of the fluorophores on the observed anisotropy. If n be far from 0 then $\vec{p_n}$ is distributed over a unit sphere uniformly and randomly but if n be at a distance r from 0 then $\vec{p_n}$ can only explore a solid angle of magnitude $4\pi(1 - \exp(-r/\xi))$ in the form of a cone with $\vec{p_0}$ as the axis. Inside that cone $\vec{p_n}$ is distributed with uniform randomness. In plotting the graph in Figure 2.6 we have normalised the anisotropy so that a very dilute solution of fluorophores always yields unit anisotropy. Let us represent the results of our simulation by the function F: the anisotropy of a distribution of fluorophores, much larger in extent than R_0, and of concentration q, is given by $F(q, \mathrm{J})$, where ξ is the length over which the orientations of the dipole moments of the fluorophores are correlated. Two features are to be noted from the plot: For dilute solutions the anisotropy drops linearly with increasing concentration of fluorophores. And whatever be the correlation length ξ, the graph begins to deviate sharply from linearity near the point q = 2. These observations will play an important role in understanding the distribution of GPI-anchored proteins on the cell membrane.

2.3 Aims of the experiment

There are proteins which fluoresce naturally — green, cyan and yellow fluorescent proteins (GFP, CFP and YFP) have been used to probe the molecular organisation at the surface of the cell. However, the tissues we are interested in do not naturally express these fluorescent proteins, so we have transfected the cells under investigation to present the fluorescent probes to the extracellular medium and to tether those probes to the plasma membrane by a GPI-anchor. Such constructs have been referred to as GFP-GPI, CFP-GPI and YFP-GPI. Furthermore, we would like to compare the behaviour of a GPI-anchored protein on the surface with that of a protein with the same ectodomain but having a different anchor. We have transfected the cell to express GFP-PIT, a protein in which the same fluorescent probe is tethered to the plasma membrane by a transmembrane domain completely different in structure from any GPI.

Obviously, we would like to study the organisation of a protein that is functional in the cell we observe, and therefore is expressed naturally by the cell. The folate receptor is the protein that has been used for this purpose. Cells have been used that express both the transmembrane isoform and the GPI-anchored isoform of the folate receptor (FR-TM and FR-GPI respectively). A fluorescent dye called PLF has been chemically bonded to the receptor. Cells have also been transfected to express FR-GFP, a construct in which GFP is bonded to the folate receptor, thus acting as a probe of the receptor. To convince ourselves that such a construct does not impede the normal function of the receptor, we measured the rate of internalisation of FR-GFP in the transfected cell and found that the rate was comparable to that of the endocytosis of FR in control cells. And transfected cells, like the control ones, internalise GPI-anchored proteins through the special compartments called GEEC (recall section 1.3), further boosting our confidence that transfection does not interfere with the processes that generate and internalise rafts.

Molecular probes such as these, deployed in mammalian tissues of different types, enabled us to tackle the following problems.

- How are GPI-anchored proteins distributed on the cell membrane? How is their distribution different from that of proteins not preferentially associated with rafts? Is this special distribution because of the lipid anchor — the GPI, or is it because of homotypic interactions among the globular proteins attached to the lipid?

- Can different kinds of GPI-anchored proteins inhabit the same raft?

- What role do the putative lipids in a raft play in the distribution of GPI-anchored proteins?

We shall address each of these questions in turn.

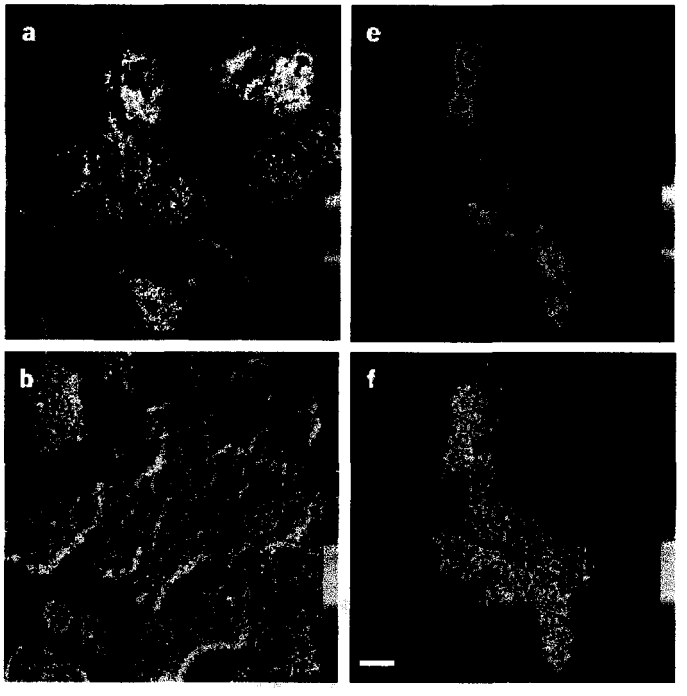

Figure 2.7: Distribution of fluorescence intensity (a,e) and fluorescence anisotropy (b,f) from a single field of cells (scale bar 20 μm). (a,b) — Constant anisotropy over a wide range of fluorescence intensity from a GPI-anchored folate receptor labeled with PLF. (e,f) — Variable anisotropy as a function of fluorescence intensity from a transmembrane isoform of the folate receptor labeled with PLF. Intensity range: black = 50 → red = 2500. Anisotropy range: black = 0.2 → red = 0.4. Reproduced from *GPI-anchored proteins are organised in submicron domains at the cell surface* (Varma and Mayor; 1998).

2.4 Organisation of the labeled protein

Upon excitation by a steady beam of polarised light, GFP-GPI on the surface of the cell exhibits constant anisotropy of fluorescence (0.295) over the entire range of intensity. The maximum intensity corresponds to approximately 400 GFP fluorophores per square micron on the cell surface. Assuming a uniform distribution on the membrane, we deduce the typical inter-protein distance to be 50 nm — much too large compared to the Forster radius (4.7 nm) for any energy transfer. Consequently with limited rotational diffusion of the fluorophore dipole moments on the membrane, we expect a constant anisotropy close to its value at infinite dilution (A, = 0.315). The observed deviation from this value indicates significant depolarisation of the fluorescence. Measurements on a GPI-anchored isoform of the folate receptor also indicate a level of depolarisation of the light emitted by a fluorophore tagged to the receptor that cannot be accounted for simply by the rotational diffusion of the protein (Figures 2.7 and 2.8).

To ascertain the causes of this depolarisation, we observe the variation of the anisotropy with time after exciting the fluorophores with a weak pulse of polarised light at the initial instant. The temporal variations of intensity and anisotropy are fitted to functions de-

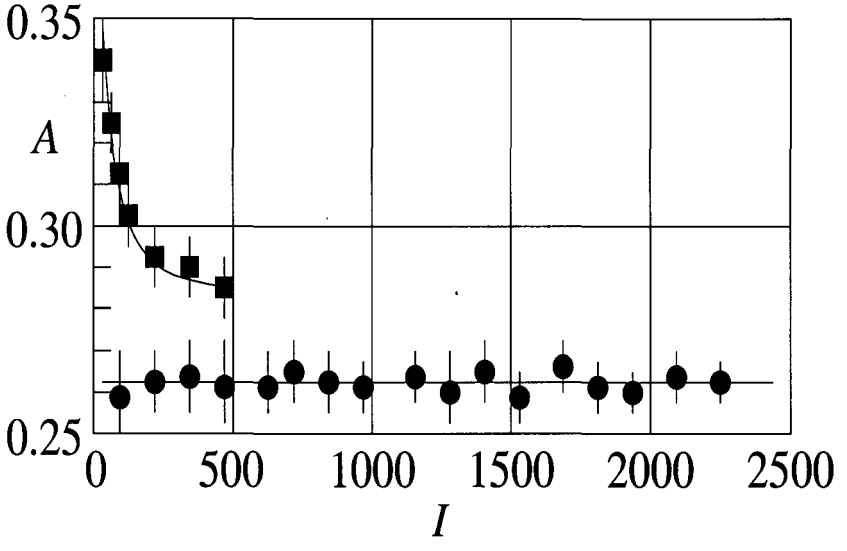

Figure 2.8: Variation of the anisotropy of fluorescence with the concentration (I, measured in arbitrary units) of the fluorophore on the cell membrane: circles — fluorophores tagged to a GPI- anchored folate receptor; squares — fluorophores tagged to a transmembrane isoform of the folate receptor.

scribed by Lakshmikanth and Krishnamoorthy (Lakshmikanth and Krishnamoorthy; 1999).

$$I(t) = \Sigma_i \alpha_i exp(-\frac{t}{\tau_i}) \tag{2.15}$$

$$\Sigma_i \alpha_i = 1 \tag{2.16}$$

$$I_{||}(t) = \frac{1}{3}(1 + 2A(t))I(t) \tag{2.17}$$

$$I_{\perp}(t) = \frac{1}{3}(1 - A(t))I(t) \tag{2.18}$$

$$A(t) = A(0)\Sigma_i \beta_i exp(-\frac{t}{\tau_i^a}) \tag{2.19}$$

$$\Sigma_i \beta_i = 1 \tag{2.20}$$

I and A are the instantaneous values of fluorescence intensity and fluorescence anisotropy respectively, $I_{||}$ and $I_{\perp}$ are the emission intensities collected at polarisations parallel and perpendicular, respectively, to the polarization of the applied excitation.

The slow components, τ_2^a and τ_3^a, are much larger than the decay time (τ_1^a) of GFP in bulk solution, undergoing rotational diffusion (Figure 2.9). Therefore the slower decay of anisotropy is because of the restricted rotation of the protein tethered to the membrane. Placing cells in a viscous medium completely eliminates the slower components confirming that they are due to the global rotation of the tethered protein. The decrease in the value of the steady state anisotropy relative to A, is thus a result of the fast component (τ_1^a). The value of τ_1^a is not changed by placing the cell in a viscous medium. This rapid decay of anisotropy indicates non-radiative transfer of energy amongst the molecules of GFP-GPI. The fast component disappears upon replacement of the GPI-anchor on GFP with a transmembrane anchor as in GFP-PIT.

protein	lifetime (ns)		anisotropy decay time (ns)		
	τ_1	τ_2	$\tau^a{}_1$	$\tau^a{}_2$	$\tau^a{}_3$
GFP in solution	2.7 {0.04} 77% (4%)	1.6 {0.2} 23% {4%}	15 {0.7}		
crosslinked GFP	2.3 {0.02} 60% {1%}	1.2 {0.01} 40% {1%}	0.3 {0.06} 30% {4%}	> 40 70% {4%}	
GFP–GPI	3.0 {0.1} 58%{11%}	1.6 {0.17} 42%{11%}	0.23 {0.11} 9% {1%}	30 {5.0} 70% {4%}	> 50 21% {4%}
GFP–PIT	2.9 (0.05) 60% (3%)	1.4 {0.07} 40% (3%)	50 {4.0}		

Figure 2.9: Anisotropy decay parameters of GFP expressed on cells of a single tissue. (Numbers in parenthesis indicate the standard deviation in the fitting parameters. Percentages correspond to the best fitting values of the amplitudes of the individual components.)

Cross-linking GFP in bulk solution results in pairing of all the molecules of the protein, the members of every pair being held a fixed distance (0.3 nm) apart. The inter-protein distance being much less than the Forster radius, we expect every chromophore of GFP to be resonating with its partner. Indeed we observe a very rapid decay of anisotropy in cross-linked GFP. Since the values of the fastest rate of decay (τ_1^a) for cross-linked GFP and for GFP-GPI on the cell membrane are equal (within experimental errors) we conclude that at least a part of the population of the GPI-anchored protein on the membrane is in dense clusters, the separation between the proteins in a cluster being of the order of 10 A.

What fraction of the population of GPI-anchored proteins on the membrane is in clusters? Can the amplitude of the fastest decay (τ_1^a) relative to the amplitude of the others $(\tau_2^a$ and $\tau_3^a)$ furnish an answer? In our experiment with a cross-linker the entire population of the protein in bulk has been cross-linked, and therefore, is effectively in "clusters". Yet the amplitude of the fastest decay of anisotropy is only 30% .

2.4.1 Density of the clustered protein

We have seen that the GPI-anchor keeps the molecules of GFP sufficiently close to one another for energy to be transferred non-radiatively among the chromophores of the pro-

tein.

Gautier and his colleagues have used a similar technique to observe the dimerisation of GFP-tagged proteins in the cytoplasm (Gautier et al; 2001). Assuming the chromophores in a pair to be separated by a distance R, they show that

$$\frac{1}{\tau^a} = 3\kappa^2 (\frac{R_0}{R})^6 \frac{1}{\tau_0} \tag{2.21}$$

where τ^a is the rate of decay of the anisotropy and τ_0 is the fluorescence lifetime. Using the values of τ^a and τ_0 for GFP-GPI given in the table and taking $\kappa^2 = 4$, its maximum value, we get R < R_0, an over-estimate of R. We have taken the fastest rate of decay for τ^a — τ_1^a in the table (Figure 2.9).

The GPI-anchor organises the protein in very dense clusters; the separation between the proteins in a cluster being less than a Forster radius.

2.4.2 Size of the cluster

When the folate receptor, a GPI-anchored protein, is labeled, in equal proportions, with a donor (fluorescein — absorbing in the green) and an acceptor (rhodamine — emitting in the red), then no red signal is detected upon shining green light on the membrane.

Assuming a cluster to be much larger than the size of a molecule, any donor in a cluster will be surrounded, in its immediate neighbourhood, by 2k fluorophores, k of which are donors and the other half acceptors. The probability of a donor transferring its energy to one of the fluorophores in the circle of its immediate neighbourhood is overwhelmingly larger than that of transferring to one beyond the circle. A donor, in its excited state, can transfer its energy through one of the following processes: (A) the energy passes to another donor, with probability p; (B) the energy passes to an acceptor, with probability q; (C) the energy is emitted spontaneously, with probability r. Obviously,

$$p + q + r = 1 \tag{2.22}$$

We shall ignore the possibility that an excited acceptor ***(A*)*** returns its energy to a donor (D). Knowing the absorption and the emission spectra of the donor and the acceptor, we find that the ratio of q to p is approximately 5. The probabilities of the individual processes can be calculated assuming pair-wise interaction between nearest neighbours $(R \sim R_0)$.

$$\text{p} = 0.1, \text{q} = 0.45, r = 0.45 \tag{2.23}$$

But a calculation that takes only an interacting pair into account grossly exaggerates the value of r because r decreases exponentially with increasing number of neighbours $(2k)$ to whom the donor can pass its energy. As a safe, albeit rough, estimate, we take

$$p = 0.15, q = 0.7, r = 0.15 \tag{2.24}$$

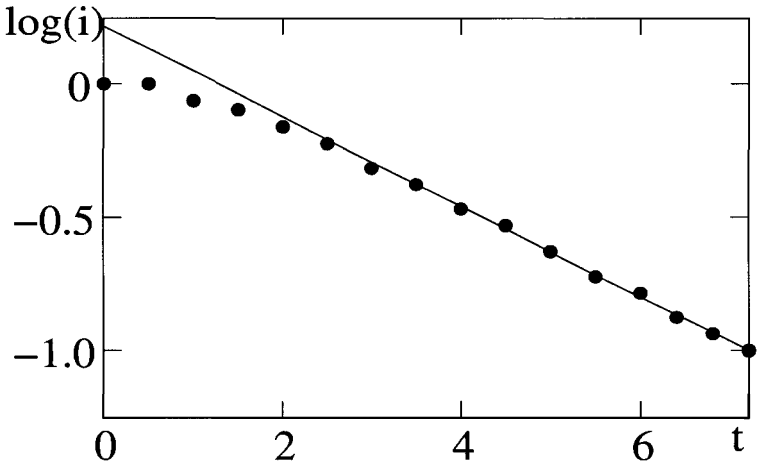

Figure 2.10: Single exponential rate of photobleaching (straight line) of FR-GPI on the cell membrane in a typical experiment. i — relative intensity after a period t (minute) of photobleaching (i = 1 at $t = 0$, the unbleached state).

We observe emission from an acceptor which has been excited by a donor. Let W be the probability that the energy of a donor (D^*)in a cluster is never transferred to an acceptor (A), then the likelihood of observing the signal is

$$Z = x(1 - W) \tag{2.25}$$

where x is the relative abundance of proteins in clusters.

In the first step after excitation, the probability of D^* not transferring to A equals the probability of D^* spontaneously emitting or D^* exciting any D. Further, the probability of D^* exciting any D equals the probability of D^* not emitting spontaneously and D^* not transferring to any A. Remember that there are k members of A within the circle of influence of D^*. Thus, in the first step after excitation, the probability of D* not transferring to A is r + a where $a = (1 - r)(1 - q)^k$.

Now if in the first step the energy was transferred to a new donor, then we do not want, in the second step, the excitation to infect an acceptor; the resultant probability amounts to r + $\alpha(r + a)$. Proceeding in this way we obtain a series of nested terms, $r + \alpha(r + \alpha(r + a(\ldots)))$ which sums to

$$W = \frac{r}{1 - \alpha} \tag{2.26}$$

Taking x = 0.2 and $k = 3$, and substituting the values of p, q and r in the expression of W, we obtain $Z = 0.17$. This value of Z represents a signal strong enough to be detected in our experiment; the threshold of detection being 10 %

What could the failure to detect any signal possibly mean? Either we have over-estimated x, the relative abundance of proteins in clusters, or our picture of a cluster as a large and uniform distribution of densely packed proteins is incorrect.

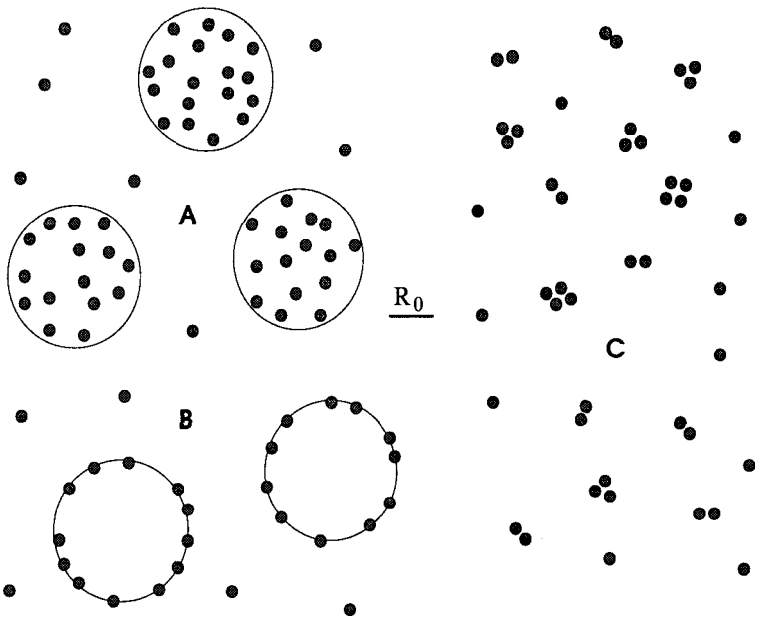

Figure 2.11: Three views of the organisation of GPI-anchored proteins (grey circles) on the cell membrane: models A, B and C.

2.4.3 Proportion of proteins in clusters

We have found that the fluorophores engaged in resonance on the cell membrane are within a Forster's radius of their intimate neighbours. Therefore q, the number of fluorophores inside a circle of radius R_0, for this system is at least 2.5. So far we have arrived at just one point in a graph. The sphere of resonance does not exceed beyond a couple of protein molecules $(100\mathring{A})$; in order to know how big or small the clusters are we have to dilute the system (increase the value of ***q)*** by destroying the fluorescence of the labels without disrupting the organisation of the proteins on the membrane.

Photobleaching, a first order chemical process, accomplishes our goal. If x_0 be the proportion of proteins outside clusters (thus $1 - x_0$ is the proportion within clusters) then the intensity of the system (normalised with respect to the unbleached state) after a period t of photobleaching is

$$i = x_0 exp(-\frac{t}{\tau_0}) + (1 - x_0) exp(-\frac{t}{\tau_c}) \qquad (2.27)$$

τ_0 and τ_c correspond to the rates of bleaching of a fluorophore outside a cluster and inside one respectively. As seen in Figure 2.10, there is only one rate of exponential decay of the population of active fluorophores — therefore photobleaching cannot distinguish a fluorophore within a cluster from one outside.

We can now begin to appreciate the nature of organisation of GPI-anchored proteins on the cell membrane from the bleaching profiles of FR-GPI: a typical case being shown in Figure 2.12. Let us first ask ourselves: are these proteins organised in dense patches $(q > 2.5)$, much larger than R_0, surrounded by isolated proteins so thinly spread over the membrane that their fluorophores hardly participate in resonance? This was the accepted

view, we call it model A (Varma and Mayor; 1998).

i, the intensity relative to the unbleached state, is the proportion of active fluorophores among all the fluorophores labeling the protein. Since the fluorophores attached to isolated proteins contribute A_n to the observed anisotropy, the anisotropy of the system normalised with respect to A_n (the anisotropy of a very dilute system, for which $i \to 0$) must be

$$a(i) = x_0 + (1 - x_0)F(qi, \xi) \tag{2.28}$$

We have an estimate of q, we set $q = 2.5$; F is the function we have met in the previous section. Now we use this equation with x_0 and ξ as the variable parameters to fit the experimental curve of Figure 2.6. The result is the curve A with $x_0 = 0.8$ and $\xi = 0.0$ as the best fitting values.

The main feature of model A is the almost constant level of anisotropy near $i = 1$. Since the clusters are very dense, an active fluorophore in a cluster will certainly find another within a Forster radius even after a moderate degree of bleaching. As a result the anisotropy remains almost fixed till the bleaching reaches a level $qi \sim 1$. The experiments, however, show a strikingly different result. The anisotropy starts rising as soon as the bleaching starts. We are thus drawn to the conclusion that even a slight bleaching suffices to rob an active fluorophore in a cluster of all its active neighbours, leaving it in an effectively isolated state. The clusters must be small.

We have also constructed a variant of model A (call it B), in which the molecules of the protein in a cluster, instead of being distributed randomly and homogeneously over the area of the cluster are localised to the periphery. As in model A, the dimension of the cluster as well as the intercluster separation are much larger than the forster radius. As a result, molecules belonging to different clusters do not engage in resonance, nor do molecules isolated from the clusters. The qualitative features of the predictions of models A and B are identical, so in the figures we compare the features of only one of them (model A) with those of model C — strikingly different from both A and B (Figure 2.11).

In model C a GPI-anchored protein is either single, not able to transfer its energy to any other molecule, or it exists as part of a cluster the size of R_0. Fluorophores belonging to separate clusters do not engage in resonance. A cluster can contain only a few proteins and every fluorophore in a cluster is within a Forster radius of every other fluorophore in that cluster. As a result, a cluster with n proteins can be characterised by $A^{(n)}$ — the anisotropy produced by a single n-mer, all the fluorophores in the cluster simultaneously exerting their influence on the energy absorbed by the cluster. Obviously, $A^{(1)} = A_n$, the anisotropy of a very dilute system of fluorophores, observed in the asymptotic limit of complete bleaching. Runnels and Scarlata have theoretically computed $A^{(n)}$ assuming that the orientations of the dipole moments of the fluorophores in a cluster are not correlated, and their results agree well with the fluorescence observed from melittin — a protein that oligomerises naturally both in aqueous solution and when bound to a lipid membrane

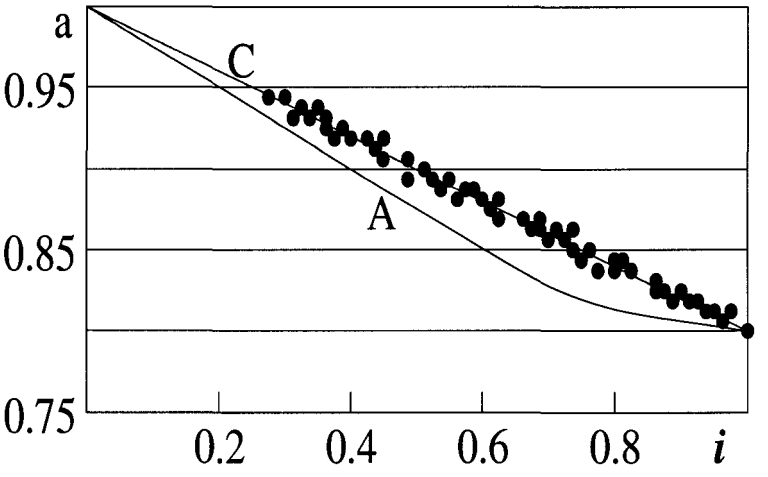

Figure 2.12: Relative anisotropy plotted against relative intensity ($i = 1$ corresponding to unbleached cells) in a bleaching experiment. A, $= 0.25$. Data from 10 cells in a typical tissue culture dish is shown. A and C are the lines that fit the data best to the theoretical models A and C.

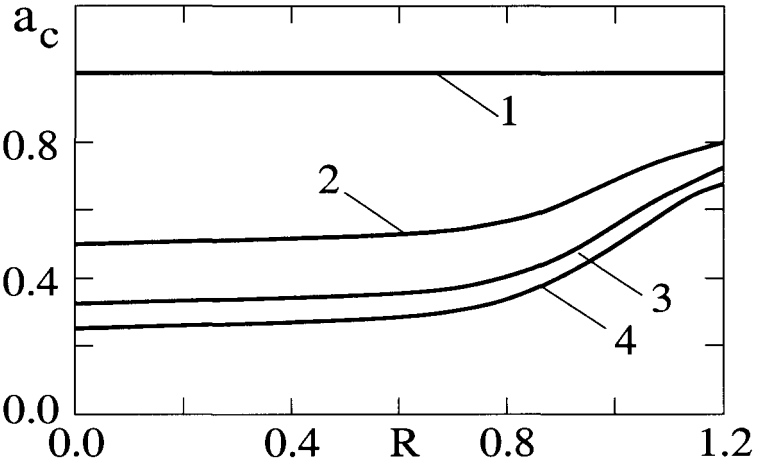

Figure 2.13: Relative anisotropy of a monomer (1), a dimer (2), a trimer **(3)** and a quadramer (4) plotted against the size (R/R_0) of the cluster (Runnels and Scarlata; 1995).

(Runnels and Scarlata; 1995). Two features are worth noting from their plot: (A) as expected, for a given size, the greater the coordination number of a cluster the smaller its anisotropy; (B) even for a very tight cluster (R << R_0) the anisotropy is not vanishingly small because the probability of the excitation returning to the initially excited molecule through multiple transfer becomes high with increasing proximity of the molecules (Figure 2.13).

Since the diameter of the globular FR is 30$\mathring{A}$, while R_0 is 70$\mathring{A}$, it is obvious that a cluster cannot contain more than four proteins. Let x_n be the proportion of proteins in clusters of coordination number n, then the proportion of isolated proteins is

$$x_1 = 1 - x_2 - x_3 - x_4 \tag{2.29}$$

In estimating the anisotropy, however, it is the proportion of proteins attached to active fluorophores that counts. Once bleaching starts, a part of the population of n-mers will

be reduced to populations of m-mers where m $= 0, 1, 2, ..., n - 1$. Let X_n denote the proportion, among all proteins — both active and dead, of those in clusters with effective coordination number n. We have seen that bleaching cannot distinguish a fluorophore inside a cluster from one without. So i, the relative intensity of the system at any instant of time, is the probability of a fluorophore still being active — be it attached to a monomer or to an n-mer. Therefore

$$X_1 = i(x_1 + (1-i)x_2 + (1-i)^2 x_3 + (1-i)^3 x_4) \tag{2.30}$$

$$X_2 = i^2(x_2 + 2(1-i)x_3 + 3(1-i)^2 x_4) \tag{2.31}$$

$$X_3 = i^3(x_3 + 3(1-i)x_4) \tag{2.32}$$

$$X_4 = i^4(x_4) \tag{2.33}$$

Note that $X_n = x_n$ for $i = 1$, the unbleached state; and $X_n \to 0$ as i $\to 0$. Let Z be the number of active fluorophores per unit area of the cell membrane, out of which Z_n belong to clusters with effective coordination number n. T is the total number of GPI-anchored proteins per unit area of the membrane, bearing fluorophores, active or dead. The anisotropy measured in the experiment must be

$$A = \frac{Z_1}{Z}A^{(1)} + \frac{Z_2}{Z}A^{(2)} + \frac{Z_3}{Z}A^{(3)} + \frac{Z_4}{Z}A^{(4)} \tag{2.34}$$

Note that

$$\frac{Z_n}{Z} = \frac{Z_n/T}{Z/T} = \frac{X_n}{i} \tag{2.35}$$

Hence, the relative anisotropy (A/A_∞) assumes the form

$$a = \frac{1}{i}(X_1 + X_2 a^{(2)} + X_3 a^{(3)} + X_4 a^{(4)}) \tag{2.36}$$

$$a^{(n)} = \frac{A^{(n)}}{A_\infty} \tag{2.37}$$

These are the expresions we have to compare our theory with experiments. The variable parameters are x_2, x_3, x_4 and $a^{(2)}$, $a^{(3)}$, $a^{(4)}$. To fix ideas let us take the simplest case: a system composed only of monomers and dimers ($x_1 + x_2 = 1$). For such a system

$$a(i) = 1 - (1 - a^{(2)})x_2 i \tag{2.38}$$

The bleaching profile is a straight line. This example brings to focus the main difference between models A and C. The anisotropy of large clusters of high density will not respond to bleaching till the system has been so diluted that neighbouring fluorophores in a cluster are more than a Forster radius apart.

Taking $a^{(2)} = a^{(3)} = a^{(4)} =$ a,, a free parameter in our model, we estimate that 20%to 40%of the population of the labeled protein on the surface is clustered (Figure 2.14).

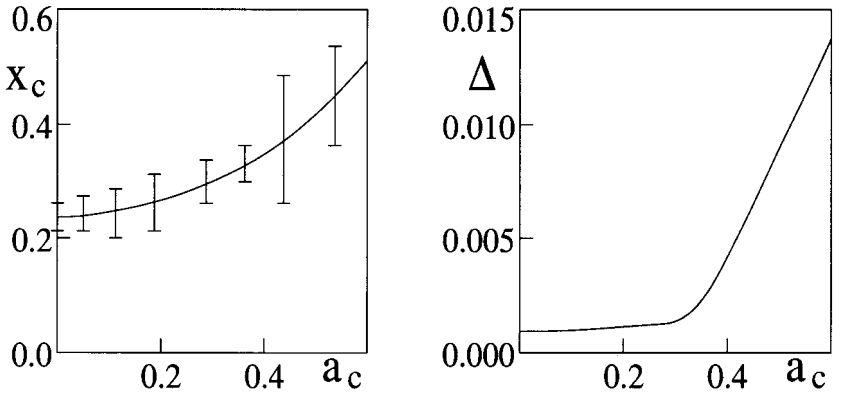

Figure 2.14: The main free parameter of model C: a,, the anisotropy of a cluster relative to the anisotropy observed at very high dilution. (L) Dependence of x,, the proportion of proteins in clusters, on *a*, — the vertical bars denote the spread in x, when the fitting is done over cells grown in 30 different dishes. (R) Dependence on a, of A, the standard deviation corresponding to the best fitting curve for cells in a typical dish, such as the one refered to in the previous figure.

2.4.4 Size of the cluster: a revised estimate

In the last section we have arrived at a new picture of a "raft": a closely held nanometre scale structure consisting of only a few molecules of GPI-anchored protein — perhaps no more than two. Now we shall use this picture in conjunction with the observation of resonance between dissimilar fluorophores attached to GPI-anchored proteins to set a strict upper limit on the number of molecules in a cluster.

Toward the beginning of this chapter (section 2.4.2), our inability to detect any signal from the acceptor upon the excitation of the donor made us skeptical of the applicability of model A. Now that model C has replaced model A, we can turn the argument of that section to reaffirm the smallness of the clusters. We shall use all the symbols introduced in section 2.4.2, their meaning unchanged. We now have

$$Z = x_2(1 - W_2) + x_3(1 - W_3) + x_4(1 - W_4) + ... \tag{2.39}$$

where W_n is the probability that the excitation of a donor in a cluster of size n is never transferred to any acceptor. For very small clusters there is considerable likelihood of a donor finding itself in a cluster without any acceptor to pass its energy to. Such a circumstance would be less probable if the strength of the population of acceptors on the membrane is increased relative to that of donors. Let us denote by d the ratio of the concentration of donors to that of acceptors. Then the relative abundance of clusters of size n consisting of m acceptors and n – m donors, amongst all clusters of size n with at least one donor is

$$P_n^m = \frac{C_m^n d^{n-m}(1-d)^m}{1-(1-d)^n} \tag{2.40}$$

To calculate W_n we split it into $(n - 1)$ parts,

$$W_n = W_n^0 + W_n^1 + W_n^2 + ... + W_n^{n-1} \tag{2.41}$$

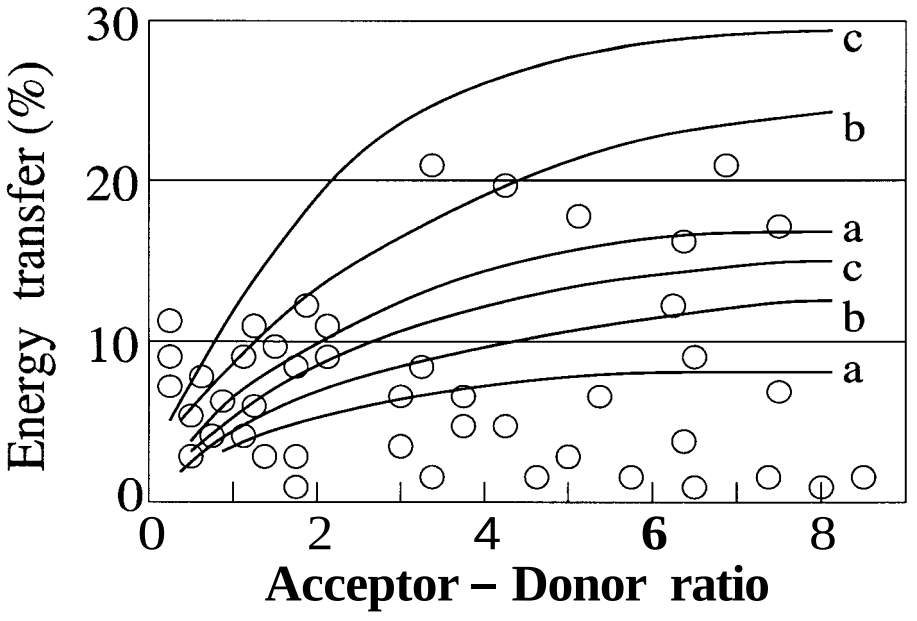

Figure 2.15: Detection of energy transfer (open dots) between CFP-GPI (the acceptor) and YFP-GPI (the donor). Lines a, b, c correspond to theoretical predictions with the clusters composed entirely of dimers, trimers and quadramers respectively; the lower and upper lines of each set correspond to 20%and 40%of the proteins being in clusters, respectively. p, q and r take the values given in equation 2.16.

where the superscript refers to the number of acceptors in the cluster. If m = 0 then certainly the donor cannot transfer its energy to any acceptor and hence

$$W_n^0 = P_n^0 \tag{2.42}$$

If m = n – 1, then the donor can spontaneously descend to its ground state unless its energy is taken by an acceptor. If the donor does not transfer its energy to any acceptor then it is a joint result of (n – 1) independent events that it does not transfer its energy to each of the (n – 1) acceptors in the cluster. As a result

$$W_n^{n-1} = P_n^{n-1}(1-q)^{n-1} \tag{2.43}$$

For intermediate values of m the calculation of W_n^m proceeds exactly along the lines laid down in section 2.4.2. We have

$$W_n^m = P_n^m(\frac{'}{1-\alpha}) \tag{2.44}$$

$$\alpha = (1-r)(1-q)^m \tag{2.45}$$

In our experiment if Z falls below 0.1 then any signal from the acceptors will be masked by noise. Since we already know that only 20 %to 40 %of the GPI-anchored proteins are clustered ($0.6 < x_1 < 0.8$), the extremely meagre signal from the acceptors (Figure 2.15) proves that the clusters consist of no more than four molecules of the protein, very likely, the clusters are dimers.

2.5 Coexistence of proteins in a cluster

The ability of GPI-anchored proteins to cluster is due to the special lipid tethering the protein to the membrane, the particular nature of the protein attached to the GPI anchor has no role to play in the formation of clusters. Molecules of different proteins tethered to the membrane by the same GPI can share one cluster.

When the folate receptor is expressed as a GPI-anchored protein on the membrane of a cell that already bears clusters of GFP-GPI the light from the GFP becomes more polarised. Molecules of the folate receptor invade the clusters of GFP, inhibiting the transfer of fluorescent energy from one molecule of GFP to a neighbouring one. Thus, judging by the anisotropy of fluorescence, it appears that a fraction of the GFP-GPI in clusters has been reduced to monomers. Two features of this rise of anisotropy upon the expression of a different GPI-anchored protein merit our attention: (A) The anisotropy increases almost linearly with the concentration of the folate receptor relative to that of the GFP, till it saturates at **A,** when all the GFP in clusters have been reduced effectively to monomers. (B) The anisotropy starts leveling off to a constant value when the concentration of the folate receptor is approximately five fold greater than the concentration of the GFP (Figure 2.16).

Let y be the concentration of the FR-GPI on the membrane, relative to the concentration of GFP-GPI, of which y_1 refers to the monomeric form of FR-GPI. Let x_1, x_2, x_3, ... denote the abundance of GFP-GPI on the membrane as monomers, dimers, trimers, ... before the expression of FR-GPI. Then the abundance of GFP-GPI that has effectively been reduced to monomers because of the coexpression of FR-GPI will be $x_1 + x_2\Delta y + x_3\Delta y^2 + \ldots$ where Ay = y – y_1. Since the major contribution to the observed anisotropy is from GFP-GPI in an effectively monomeric state, the almost linear rise of the anisotropy with increasing y clearly shows that the clusters of GPI- anchored proteins are indeed small, being primarily dimers. This exercise further corroborates the inapplicability of model A — if the clusters were much larger than the forster radius then we would expect a sigmoid shape for the graph of **A** against y — *A* being almost insensitive to increase in y till y reaches a threshold.

We have seen that approximately 20%of GFP-GPI are in clusters; we would expect a similar fraction of FR-GPI too to participate in the formation of clusters, either with itself or with GFP-GPI. Indeed the observation that the graph of A starts leveling off to ***A,*** as y approaches a value of 5, does indicate that approximately 80%of the FR- GPI exist as monomers on the cell membrane. Had the entire population of FR-GPI participated in the formation of clusters then **A** would start saturating to **A,** for much smaller values of y — around y = 1.

When the isoform of the folate receptor that is attached to the membrane by a transmembrane anchor is expressed on the cell membrane the fluorescence from GFP-GPI is not affected at all. Thus only a GPI-anchor can enable a protein to form small (nanometre

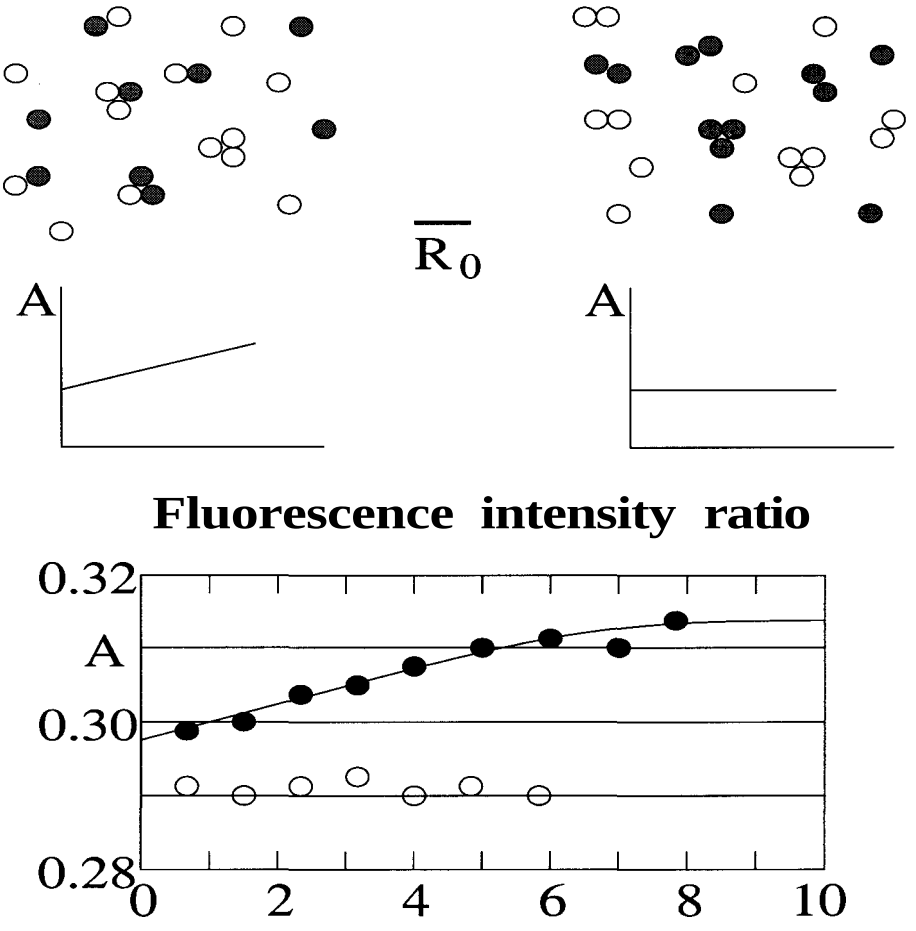

Figure **2.16:** (T) Effect on the anisotropy of fluorescence from a GPI-anchored protein (white circles) when another protein (grey circles) is also expressed on the membrane — (L) if the two proteins cohabit a cluster then the anisotropy increases with increasing ratio of the concentration of grey circles to that of white circles; (R) if the proteins form separate clusters then the anisotropy is unchanged. (B) Experimental observation of the anisotropy of fluorescence from GFP-GPI when FR-GPI is also expressed in the cell (black points); anisotropy of fluorescence from GFP-GPI when a transmembrane anchored isoform of FR is expressed in the same cell (white points).

scale) clusters.

2.6 Role of lipids in organising the proteins

Compactin interferes with the metabolism of the cell and, as a result, the level of cholesterol on the surface of the cell is lowered. If we assume that even after treatment with compactin GPI-anchored proteins on the surface is present in clusters and as isolated monomers, then we can apply model C to the results of the bleaching experiment, precisely the way we did in the previous section. While the best fitting values of x_1, the proportion of proteins in the isolated state, were in the range **0.6** to **0.8** for control cells, the range was **0.65** to **0.9** for cells treated with compactin (Figure 2.17). Therefore the organisation of GPI-anchored proteins is mediated by the level of cholesterol in the mem-

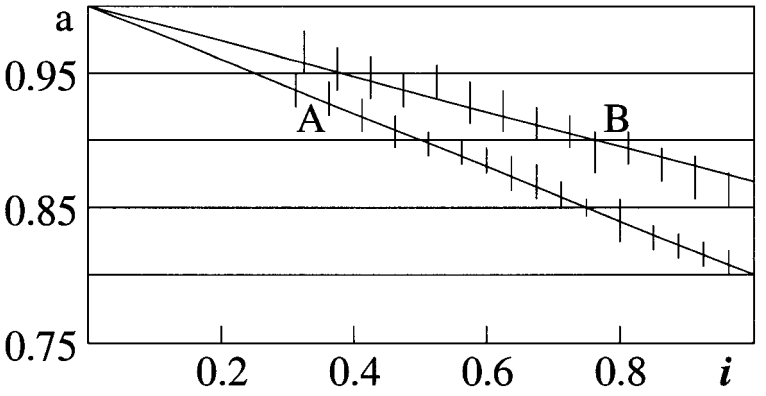

Figure 2.17: Profiles of photobleaching a fluorophore attached to a GPI-anchored folate receptor in (A) control cells and (B) cells treated with compactin. (Compare Figure 2.12.) The bars denote the spread in the anisotropy over 15 cells for identical range of values of the relative intensity.

brane.

Saponin, on the other hand, acts directly on the surface of the cell and extracts cholesterol from the bulk of the lipid bilayer. Upon the action of saponin the fast component of the decay of anisotropy of the fluorescence of GFP-GPI, when excited by a pulse of polarised light, completely disappears (compare Figure 2.9). While τ_1^a took a value of 0.23 nanosecond in control cells, it jumps to 40 nanosecond for cells treated with saponin. Therefore the dense clusters of proteins on the surface of the cell are removed by saponin.

The removal of cholesterol dissociates an appreciable fraction of clusters. The removal of glycosphingolipids, even by drastic amounts, does not affect the clusters, but facilitates the removal of cholesterol — the relative anisotropy (a) at an unbleached state $(i = 1)$ took a value of 0.87 for cells treated with compactin, but a increased to 0.91 when the cells were depleted of cholesterol after the depletion of sphingolipids. Based on these observations, we draw a picture of domains on the membrane, rich in cholesterol and sphingolipids, most of the GPI-anchored proteins in those domains being oligomerised, while isolated monomers of GPI- anchored proteins dwell in the rest of the membrane.

2.7 Towards a super-organisation

Our analysis of the experimental observations has been based on the premise that the life of a cluster spans much beyond the period of fluorescence of the labeling dye. However a cluster of proteins on the cell membrane is not a permanent entity; in concordance with the report of Subczynski and Kusumi, we expect the lifetime of a cluster to be of the order of a millisecond (Subczynski and Kusumi; 2003). Since a free lipid molecule diffuses over the entire membrane in an interval of the order of a second, we would expect the clusters and the isolated GPI-anchored proteins to be in thermal and chemical equilibrium. But that is not the case.

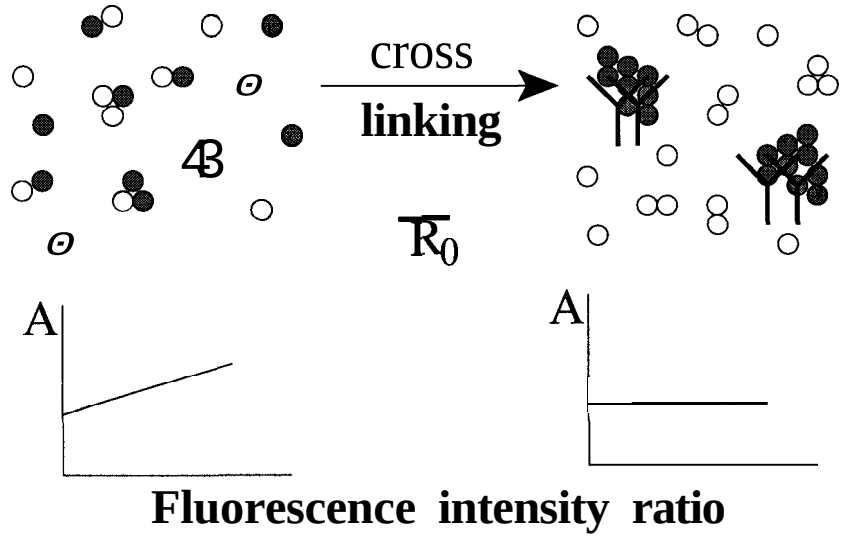

Figure 2.18: Cross-linking of one kind of GPI-anchored protein (grey circles) in a mixture of several segregates it and allows the rest (white circles) to reorganise the clusters. (Compare Figure 2.16.)

2.7.1 Non-equilibrium nature of the cluster

For simplicity, let us assume that the clusters are all in the form of dimers. Then $\frac{x_2}{2}$ is the number of clusters per unit area of the membrane. Assuming the distribution of proteins on the membrane to be in equilibrium, we may apply the law of mass action to this system of monomers and dimers. The rate of dissociation of the dimers is equal to $k_2(\frac{x_2}{2})$ while the rate of aggregation of a pair of isolated proteins to yield a dimer is equal to $k_1 x_1^2$ where $\mathrm{K} = \frac{k_1}{k_2}$ is the equilibrium constant of the reaction. These rates must balance one another in equilibrium; so we get

$$\frac{x_2}{2} = K x_1^2 \tag{2.46}$$

However, the observation that the anisotropy of fluorescence of GPI-anchored proteins is independent of the levels of expression of the protein over a ten fold range (Figures 2.7 and 2.8) implies, from our analysis of model C, that the ratio of x_2 to x_1 is constant over this range. Our assumption that the monomers and the dimers mix freely with one another and reach a state of equilibrium has led us to conflict with the reality. There must be regions on the membrane where dimerisation is actively promoted or actively prevented, disrupting the overall balance of the dissociation of dimers and the aggregation of monomers though we are unable to know the size or the constitution of those regions.

2.7.2 Dynamic nature of the cluster

When two kinds of GPI-anchored proteins (A and B) are coexpressed in the cell we have seen that they produce mixed clusters. When A is segregated from the clusters by cross-linking with an antibody that specifically binds A then patches of A, but not of B, are

seen on the membrane. Therefore the clusters are labile, **A** completely dissociates from B upon cross-linking. The interaction between proteins in a cluster must be much weaker than the strength of the covalent bond between an antibody and its target protein.

Once **A** is torn away from the clusters, B behaves as if **A** was never its partner in a cluster! B reorganises itself into its own clusters, the anisotropy of its fluorescence is again independent of its concentration on the membrane. The steady state value of the anisotropy is the original value, when **A** was not expressed at all (Figure 2.18).

Therefore the regions of the membrane which confine most or all of the clusters and prevents the equilibration of clusters and monomers are not disrupted by the process of crosslinking. Henceforth we shall call these regions rafts. A raft spawns clusters of GPI-anchored proteins and so it must be bigger than a cluster. We do not know, however, does a patch of cross-linked protein break away from its parent raft or does it stimulate the raft to grow around the patch?

2.7.3 A priori and induced structures

Upon crosslinking a species of GPI-anchored proteins with an antibody the crosslinked patches separate from the rafts bearing the unperturbed species. The clusters induced by crosslinking are endocytosed through the clathrin-mediated pathway, not through the route by which rafts enter the cell. Therefore the nanoscale clusters of proteins we have observed on the surface of the cell form an a priori organisation on their own in which the size of each cluster is maintained within a strict upper bound. These a priori organisations, though open to external perturbations, has the property of homeostasis — expelling large induced structures to regulate its internal environment within specific limits. Thus rafts, bearing GPI-anchored proteins of multiple types, can coalesce with one another to form bigger organisations but without sacrificing the special internal constitution of its proteins.